PHYSICAL REVIEW B **85**, 155433 (2012)

# Skipping and snake orbits of electrons: Singularities and catastrophes

Nathan Davies,[1] Aavishkar A. Patel,[1,2] Alberto Cortijo,[1,3] Vadim Cheianov,[1] Francisco Guinea,[4] and Vladimir I. Fal'ko[1]
[1]*Physics Department, Lancaster University, Lancaster LA1 4YB, United Kingdom*
[2]*Department of Physics, Indian Institute of Technology Kanpur, Kanpur 208016, India*
[3]*Departamento de Física Teórica, Universidad Autónoma de Madrid, 28049 Madrid, Spain*
[4]*Instituto de Ciencia de Materiales de Madrid, CSIC, 28049 Madrid, Spain*
(Received 25 February 2012; published 16 April 2012)

Near the sample edge, or a sharp magnetic field step, the drift of two-dimensional (2D) electrons in a magnetic field has the form of skipping and snake orbits. We show that families of skipping and snake orbits of electrons injected at one point inside a 2D metal generically exhibit caustics folds, cusps, and cusp triplets, and, in one exceptional case, an extreme section of the butterfly bifurcation. Periodic appearance of singularities along the $\pm B$ interface leads to the magneto-oscillations of nonlocal conductance in multiterminal electronic devices.

DOI: 10.1103/PhysRevB.85.155433 PACS number(s): 73.23.−b, 05.45.−a, 05.60.Cd, 73.43.Qt

Skipping orbits were introduced into the physics of metals by Niels Bohr in the early studies of diamagnetism.[1] They also play a special role in the two-dimensional (2D) electron systems, by determining the chiral current-carrying properties of the electron edge states[2] in the quantum Hall effect.[3] Snake orbits have been discussed, first, in the context of the electrons propagation along domain walls in ferromagnetic metals[4,5] and, later, used for channeling ballistic electrons in 2D semiconductors in a spatially alternating magnetic field,[6–11] $\mathbf{B} = \mathbf{l}_z B \mathrm{sign} x$. In isotropic 2D metals, where all electrons with energies close to the Fermi level revolve along cyclotron circles with the same radius, $R = p_F/eB$, skipping and snake orbits have the form of consecutive circular segments matched by the specular reflection at the edge, or by the smooth continuity on the opposite sides of the $\pm B$ interface; see Fig. 1. A close relation between these two families can be established[12] by folding a sheet of a 2D material (e.g., graphene,[13] which can sustain sharp bends) in a homogeneous magnetic field. The electron path near the fold looks like a skipping orbit with circular segments alternating between the top and bottom layers, but, when projected onto an unfolded sheet, the electron motion resembles the motion near a $\pm B$ interface.

Below, we study bunching in the families of skipping and snake orbits of electrons injected into a 2D metal from a pointlike source and singularities in the spatial distribution of electronic trajectories. Mathematically, such features originate from the singularities in the differentiable maps in Thom's catastrophe theory.[14,15] Caustic folds and bifurcation cusps are the most common singularities, which are often encountered in ray optics[16] and responsible for sunlight sparkling on the sea or twinkling starlight.[17] In electronics, observations of caustics are less common. Caustics and focusing of surface-band electrons have been observed in "corals" built by the STM manipulation of atoms on noble-metal surfaces,[18] and, inspirationally for this work, one family of caustics has been identified[19] for skipping orbits of electrons injected from a point contact into a 2D electron gas in GaAs/AlGaAS heterostructures.[20–23] Here, we demonstrate that caustic bunching is generic for snake/skipping orbits of electrons injected into a 2D metal at any distance $X_0 < 2R$ near the $\pm B$ interface/sample edge. For $X_0 > R > \frac{1}{2}X_0$, Fig. 1, the networks of caustics display a periodic appearance of individual cusps, which split into cusp triplets when $R > X_0$. In general, such crossover would happen via the formation of swallowtail singularities,[16] but, uniquely for a sharp field step/sample edge, these two regimes are separated, at $X_0 = R$, by a 4th-order unstable singularity which represents an extreme section of the butterfly bifurcation known in the catastrophe theory of surfaces in higher-dimensional spaces.[24]

For electrons isotropically injected into a 2D metal with an isotropic dispersion of electrons, at a point $(-X_0,0)$ near the $\pm B$ interface/edge at $x = 0$, their trajectories can be parametrized using the angle $\theta$ (counted in the anticlockwise direction) between the initial velocity and the $y$ axis. In Fig. 1, these trajectories are drawn for $0 < \theta < 2\pi$, with a step of 0.1. For the orbits near the $\pm B$ interface/edge, these are the sequences of semicircles with the coordinates $\mathbf{r}_n = (x_n, y_n)$,

$$x_n = \zeta_n + R\sin\varphi, \quad \zeta_n = \gamma^n(R\cos\theta - X_0),$$
$$y_n = \eta_n + R\cos\varphi, \quad \eta_n = 2n\sqrt{R^2 - \zeta_0^2} + R\sin\theta,$$

where $n = 0,1,2,...$ labels the number of times the trajectory arrived at the interface/edge at $x = 0$, angle $\varphi$ counted from the $y$ axis allows one to describe all points on a single segment ($\gamma^n R\sin\varphi < -\zeta_0$, for $n > 0$), and $\gamma = +1/-1$ for skipping/snake orbits. A sheet density,

$$\rho = \int \delta(\mathbf{r} - \mathbf{r}_n) d\varphi d\theta,$$

of such trajectories can be evaluated (using a sequence of substitutions) as

$$\rho(\mathbf{r}) = [1 - \gamma^n \mathrm{sign} x] \left|\frac{\partial F}{\partial\theta}\right|^{-1}\Bigg|_{F=0}, \tag{1}$$

$$F(x,y;\theta,R) \equiv (x - \zeta_n)^2 + (y - \eta_n)^2 - R^2. \tag{2}$$

This density is singular along caustics $\mathbf{R}_n = (u_n, v_n)$, where, simultaneously,

$$\frac{\partial F}{\partial\theta} = 0 \quad \text{and} \quad F = 0. \tag{3}$$

 

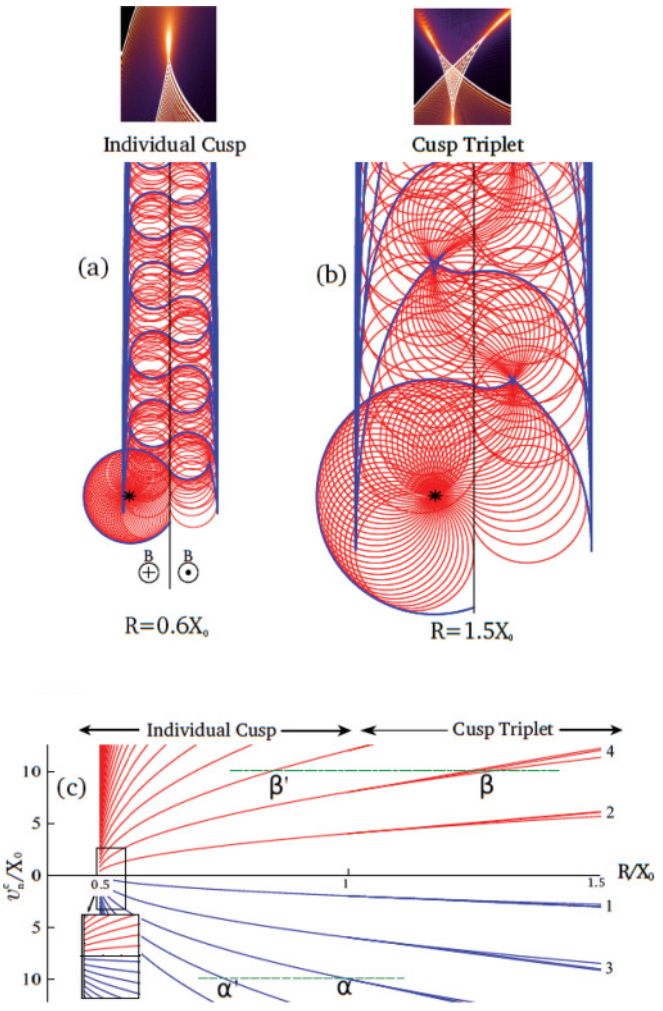


FIG. 1. (Color) Caustics (blue) of snake orbits (red) for electrons injected at a distance $X_0$ from the $\pm B$ interface: (a) $R < X_0$; (b) $R > X_0$. A little star shows the position of the injector on the $x$-$y$ plane, and the vertical line, the $\pm B$ interface at $x = 0$. (c) Positions, $v_n^c$ of cusps on the right-hand side (bottom) and left-hand side (top) from the $\pm B$ interface. Top panels: Semiclassically calculated interference patterns in the vicinity of classical singularities.

This determines the equations for caustics,

$$u_n = \zeta_n \pm R\frac{c_n s}{\sqrt{1+c_n^2}}, \quad c_n = \frac{2n\zeta_0}{\sqrt{R^2-\zeta_0^2}} + \cot\theta,$$
$$v_n = \eta_n \pm R\frac{\gamma^n s}{\sqrt{1+c_n^2}}, \quad s = -\text{sign}(\sin\theta), \tag{4}$$

where we choose the sign "±" and permitted range of $\theta$ using the requirement that

$$\zeta_0\sqrt{1+c_n^2} \pm \gamma^n c_n s R < 0.$$

These caustics can be viewed as projections of the folds of a 2D surface $F(x,y;\theta) = 0$ in the space $x,y,\theta$ onto the $x$-$y$ physical coordinate plane.

The density of trajectories is most singular in the vicinity of cusps, with the tips located at the points $(u_n^c, v_n^c)$, which are projections of the regions where two oppositely curved folds on the surface $F(x,y;\theta = 0)$ merge together, flattening the wrinkles. The tip of the cusp is characterized by the condition $d^2F/d\theta^2 = 0$, additional to Eq. (3). This was used, together with Eqs. (4), both for analytical determination of the form of caustic cusps and for numerical plotting of caustics in Fig. 1 for strong and weak magnetic fields. Also, catastrophe theory can be applied to the analysis of the interference of waves resulting in characteristic patterns in the vicinity of singular points of the distribution of classical trajectories;[17,25] we show such generic interference patterns in the top insets in Figs. 1(a) and 1(b).

For a strong magnetic field, such that $X_0 > R > \frac{1}{2}X_0$, the periodically appearing cusps are illustrated in Fig. 1(a), with universal curving of caustics near the tip of the cusps,

$$u_n - u_n^c \propto \pm\left(v_n^c - v_n\right)^{3/2}, \quad u_n^c = -\gamma^n X_0. \tag{5}$$

The $y$ positions of the cusps $v_n^c$ are plotted in Fig. 1(c) against the ratio $R/X_0$. The top/bottom parts of Fig. 1(c) distinguish between the cusps appearing on the left/right from the magnetic field step. For skipping orbits, the latter should be folded onto the same half-plane. When $R < \frac{1}{2}X_0$, all the extended caustics disappear, leaving only one limiting caustic of the closed orbits: a circle with a $2R$ radius centered at the source. The inset in Fig. 1(c) shows the limiting positions of the cusps at $R \to \frac{1}{2}X_0$ (spaced with the period of $\approx 0.4X_0$) before their final disappearance.

The second regime in the formation of catastrophes of snake/skipping orbits is characteristic of the weak magnetic fields, such that $R > X_0$. In this case, cusp singularities appear in triplets, as shown in Fig. 1(b), and their positions are shown on the right-hand side of Fig. 1(c). Note that for $X_0/R \to 0$ caustics in Fig. 3(b) transform into caustics of skipping orbits originated from a point source exactly at the edge of a 2D system.[19] The semiclassically calculated interference pattern of the electron waves in the vicinity of the cusp triplets is illustrated in the top inset in Fig. 1(b).

The cusp triplets in Fig. 1(b) are typical for the section of a butterfly caustic surface,[16,24] for which the most singular critical section is realized when $R = X_0$, Fig. 2. The butterfly singularity is usually associated with a 4-dimensional surface, described by a polynomial equation,

$$F(z;a,b,c,d) = z^5 - az^3 - bz^2 - cz - d = 0, \tag{6}$$

in the vicinity of the origin of a 5-dimensional space with coordinates $(z,a,b,c,d)$. In the context of skipping/snake orbits, Eqs. (2) and (6) are related by the substitution

$$z = \theta + \frac{2nR - y}{5X_0} + \frac{x + \gamma^n X_0}{30nX_0},$$
$$a = \frac{2y + 8nR}{3nX_0} - 4, \quad b = \frac{2(x + \gamma^n X_0)}{nX_0}, \tag{7}$$
$$c = \frac{4(y - 2nR)}{nX_0}, \quad d = -2b.$$

The coordinates $x$ and $y$, plus parameters $\theta$ and $R/X_0$, select a 4-dimensional section of such a 5-dimensional space, whereas at the transition between the two regimes of caustics, $R = X_0$, relations in Eq. (7) select an even more peculiar section of a generic surface described by Eq. (6): a pair of folds on a surface in the space $(x,y,\theta)$ which merge together at the point where $d^N F/d\theta^N = 0$, with $N = 1,2,3,4$. Projected onto the

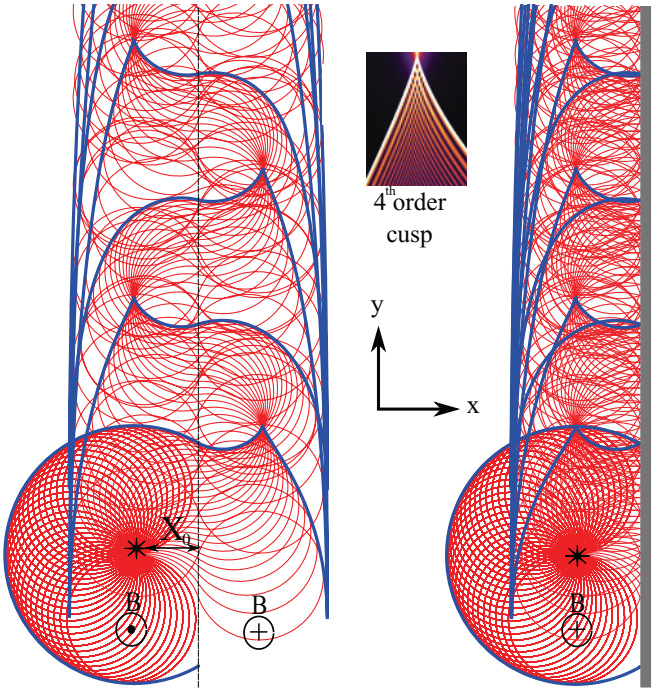


FIG. 2. (Color) Snake orbits (left) and skipping orbits (right) for electrons injected at a distance $R = X_0$ from the $\pm B$ interface/edge, with caustics (blue) merging at a "4th-order cusp": a 2D section of the 4-dimensional "butterfly" caustic surface in a 5-dimensional space.[16,24] Inset shows the interference pattern in the vicinity of such 4th-order cusp.

$x$-$y$ plane, this pair of folds can be seen as a caustic bifurcation (4th-order cusp), Fig. 2, with

$$u_n - u_n^c = \pm\left(\frac{4}{5}\right)^{5/4} \frac{\left(v_n^c - v_n\right)^{5/4}}{(nR)^{1/4}},$$
$$u_n^c = -\gamma^n X_0, \quad v_n^c = 2nX_0. \tag{8}$$

The above results are also applicable to the electron skipping orbits, by folding caustics of snake orbits onto a single half plane, as shown on the right-hand side of Fig. 2.

Although the butterfly catastrophe would be a stable singularity for the families of rays in high-dimensional spaces,[14–17,24] it is not stable in 3 dimensions $(x,y,\theta)$. Its formation, with a peculiar bifurcation described by Eq. (9), is peculiar for an infinitely sharp $\pm B$ interface. Any weak smearing of the interface, or an effective gauge field created for electrons by lattice deformations, e.g., in a bent region of a folded graphene sheet,[26] replaces it by a precursive formation of a weaker singularity somewhere near the already existing cusp—a "swallowtail" catastrophe[16,24]—consisting of the nucleation of a pair of cusps, followed by gradual separation of the latter until the cusps form the triplets shown in Fig. 1(b). Nevertheless, a reminiscence of the higher-order singularities may be picked up by a finite-radius local probe detecting a higher density of electrons injected from a pointlike source in one of the experimental setups proposed below.

The periodic appearance of cusps of snake and skipping orbits suggests that they can generate classical magneto-oscillation of conductance in ballistic multiterminal devices

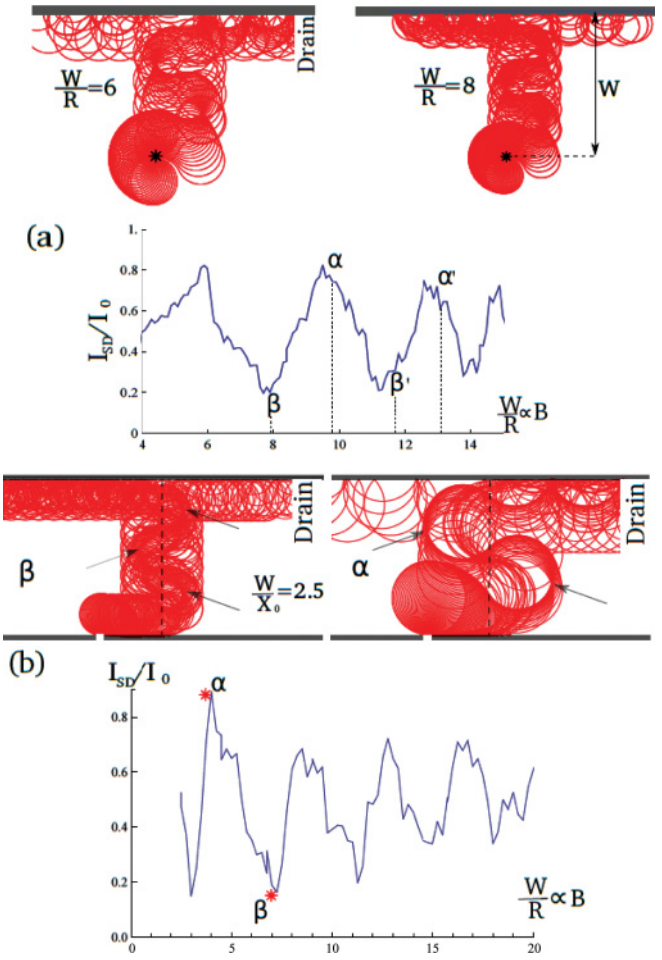


FIG. 3. (Color online) (a) Bunching of trajectories (for $X_0 = R$) and the calculated magneto-oscillations of the current $I_{SD}$ in the three-terminal geometry (for $W = \pi^2 X_0$). Here, the injected current is registered in the drain placed on the right from the $\pm B$ field step. The marks $\alpha,\alpha'/\beta,\beta'$ relate maxima/minima of $I_{SD}$ to the cusps reaching the upper edge of the sample on the right/left from the field step, as marked on Fig. 1(c). Here, oscillations of current are plotted against the dimensionless ratio $W/R = BeW/p_F$, which is the same as magnetic measured in units of $p_F/eW$, and, thus, represent the form of measureable magneto-oscillation. (b) Bunching of trajectories and magneto-oscillations of the source-drain current in a four-terminal device with a $\pm B$ interface and width $W$. Two top panels illustrate families of trajectories for the conditions corresponding to the maximum/minimum ($\alpha/\beta$) of $I_{SD}$, with positions of the cusps pointed by arrows. The smaller and faster oscillations of current in (a) and (b) are the artifact of numerical procedure.

incorporating a $\pm B$ interface (or graphene fold in a magnetic field). Figure 3 shows the calculated magneto-oscillations of electrical current for two geometries of such devices. In Fig. 3(a) we plot the magnetic-field-dependent fraction, $I_{SD}/I_0$ of the current $I_0$, injected from a point contact near the $\pm B$ interface, which reaches the drain on the right-hand side of the edge. This was calculated by following the propagation of each of the injected electrons for the time up to $10W/v_F$ (where $W$ is the distance from the source to the upper edge). Such a cutoff in the length of electronic trajectories mimics the effect

of a finite mean-free path, $\ell \sim 10W$. The large oscillations in $I_{SD}$ are the result of singularities in the ensemble of the electron trajectories: Each time when a cusp on the right from the interface reaches the upper sample edge, $I_{SD}$ experiences a maximum, and when a singularity on the left reaches the sample edge, a minimum. Such oscillatory behavior persists both in the regime of individual cusp formation and the regime of cusp triplets. However, for the lowest magnetic fields, such that $R/X_0 \ll 1$, the cusps in each triplet get separated so much that one of them crosses the $\pm B$ interface; after that, the magneto-oscillations of $I_{SD}$ become rather irregular and loose in the amplitude. Figure 3(b) gives an example of magneto-oscillations of the current $I_{SD}$ in a 4-terminal device incorporating a $\pm B$ interface. Here, current is injected from an isotropic side contact at the lower edge (biased against the electrode on the left-hand side at the upper edge) and registered using a drain contact placed at the right-hand side at the upper edge. Similarly to Fig. 3(a), oscillations of $I_{SD}$ in Fig. 3(b) reflect the periodic appearance (on the left- and right-hand sides from the $\pm B$ interface) of cusps in the family of sequentially linked skipping and snake orbits. The magneto-oscillations of source-drain current in Fig. 3 demonstrate a characteristic behavior, whose details depend on the value of $W/X_0$.

To summarize, we show that snake/skipping orbits of electrons injected at one point into a 2D metal (at the distance $X_0$ from the $\pm B$ interface/edge) generically display caustic bunching and formation of intense local singularities—cusps—with two characteristic regimes of cusp formation: (i) the periodic appearance of individual cusps (for $2R > X_0 > R$) and (ii) cusp triplets (for $R > X_0$). Singularities in the distribution of trajectories, which are most intense when $R = X_0$, can lead to the classical magneto-oscillations in the nonlocal conductance of multiterminal devices made, e.g., of a bifolded graphene flake. Alternatively, one can employ near-field optics to generate electron-hole pairs in the heterostructure, with electrons placed at the energy close to the Fermi level, and, then, to detect the presence of singularities by measuring magnetic-field and source-position dependencies of a voltage drop between a fixed point contact and a massive contact placed farther up along the edge.

The authors thank I. Aleiner for useful discussions, and the Royal Society and EPSRC for financial support.

[1] N. Bohr, in *Niels Bohr Collected Works* (Elsevier, Amsterdam, 1972) Vol. 1, p. 276.
[2] E. Teller, Z. Phys. **67**, 311 (1931).
[3] B. I. Halperin, Phys. Rev. B **25**, 2185 (1982).
[4] R. G. Mints, JETP Letters - USSR **9**, 387 (1969).
[5] R. Shekhter and A. Rozhavski, Solid State Commun. **12**, 603 (1973).
[6] J. E. Müller, Phys. Rev. Lett. **68**, 385 (1992).
[7] J. Reijniers and F. M. Peeters, J. Phys.: Condens. Matter **12**, 9771 (2000).
[8] J. Reijniers, A. Matulis, K. Chang, F. M. Peeters, and P. Vasilopoulos, Europhys. Lett. **59**, 749 (2002).
[9] T. Vancura, T. Ihn, S. Broderick, K. Ensslin, W. Wegscheider, and M. Bichler, Phys. Rev. B **62**, 5074 (2000).
[10] D. N. Lawton, A. Nogaret, S. J. Bending, D. K. Maude, J. C. Portal, and M. Henini, Phys. Rev. B **64**, 033312 (2001).
[11] M. Cerchez, S. Hugger, T. Heinzel, and N. Schulz, Phys. Rev. B **75**, 035341 (2007).
[12] D. Rainis, F. Taddei, M. Polini, G. León, F. Guinea, and V. I. Fal'ko, Phys. Rev. B **83**, 165403 (2011).
[13] K. S. Novoselov, A. K. Geim, S. V. Morozov, D. Jiang, M. I. Katsnelson, I. V. Grigorieva, S. V. Dubonos, and A. A. Firsov, Nature (London) **438**, 197 (2005).
[14] R. Thom, *Structural Stability and Morphogenesis* (Benjamin Press, Reading, MA, 1975).
[15] V. I. Arnold, *Singularities of Caustics and Wave Fronts*, Mathematics and Its Applications (Springer, Berlin, 2002).
[16] Singularities encountered in this work have the following standard representation in the classification of catastrophes (Refs. 15 and 16): caustics ($A_2$), cusps ($A_3$), swallow tail ($A_4$), and butterfly ($A_5$).
[17] M. Berry, Adv. Phys. **25**, 1 (1976).
[18] H. C. Manoharan, C. P. Lutz, and D. M. Eigler, Nature (London) **403**, 512 (2000).
[19] C. W. J. Beenakker, H. Van Houten, and B. J. van Wees, Europhys. Lett. **7**, 359 (1988).
[20] H. van Houten, B. J. van Wees, J. E. Mooij, C. W. J. Beenakker, J. G. Williamson, and C. T. Foxon, Europhys. Lett. **5**, 721 (1988).
[21] V. J. Goldman, B. Su, and J. K. Jain, Phys. Rev. Lett. **72**, 2065 (1994).
[22] J. H. Smet, D. Weiss, R. H. Blick, G. Lütjering, K. von Klitzing, R. Fleischmann, R. Ketzmerick, T. Geisel, and G. Weimann, Phys. Rev. Lett. **77**, 2272 (1996).
[23] K. E. Aidala, R. E. Parrott, T. Kramer, E. J. Heller, R. M. Westervelt, M. P. Hanson, and A. C. Gossard, Nature Physics **3**, 464 (2007).
[24] Yu. A. Kravtsov and Yu. I. Orlov, *Caustics Catastrophes and Wave Fields* (Springer, Berlin, 1999).
[25] M. Berry, in *Chaotic Behavior of Deterministic Systems*, edited by G. Iooss, R. Hellemenn, and R. Stora (North Holland Publishing, 1983), p. 173.
[26] M. Vozmediano, M. Katsnelson, and F. Guinea, Phys. Rep. **496**, 109 (2010).